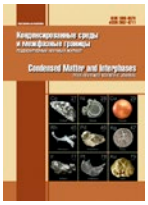

ISSN 1606-867X (Print)
ISSN 2687-0711 (Online)
Condensed Matter and Interphases
Kondensirovannye Sredy i Mezhfaznye Granitsy
https://journals.vsu.ru/kcmf/

Review

Review article
https://doi.org/10.17308/kcmf.2024.26/12398

Phases with layered (AB) and "defective" (A_2B_3) structures in A^{III}–B^{VI} systems
Part 1. Structural uniqueness and properties of bulk samples and films. Review

A. Yu. Zavrazhnov[1]✉, N. Yu. Brezhnev[2], I. N. Nekrylov[1], A. V. Kosyakov[1], V. F. Kostryukov[1]

[1]*Voronezh State University,*
1 Universitetskaya pl., Voronezh 394018, Russian Federation

[2]*Voronezh State Agricultural University,*
1 Michurin st., Voronezh 394087, Russian Federation

Abstract

The review analyses and, where possible, reconciles data on two large groups of inorganic substances that are very unusual in terms of structure and properties, designated as $A^{III}B^{VI}$ compounds. The structures and properties of typical compounds of these systems: $A_1^{III}B_1^{VI}$ and $A_2^{III}B_3^{VI}$ were considered. The relationship between the structure and the nature of the chemical bond and the organization of stoichiometric vacancies in crystal lattices is described in detail. The genesis of structures was analyzed for various modifications of $A_2^{III}B_3^{VI}$ sesqui-chalcogenides. The transformations of these compounds into each other were also considered in relation with the ordering/disordering processes of stoichiometric vacancies. The possibilities of forming nanolayer structures, tubulenes, and intercalates were demonstrated for $A_1^{III}B_1^{VI}$ layered compounds. The prospects for the application of both nanolayer coatings and bulk single crystals of $A_1^{III}B_1^{VI}$ and $A_2^{III}B_3^{VI}$ phases were analyzed. The presented review is based on the analysis of both literary data and the results of the studies of the authors and some other researchers of Voronezh State University.

Keywords: Gallium chalcogenides, Indium chalcogenides, Stoichiometric vacancies, Polymorphism, Vacancy ordering, Epitaxy, Layered structure

For citation: Zavrazhnov A. Y., Brezhnev N. Y., Nekrylov I. N., Kosyakov A. V., Kostryukov V. F. Phases with layered (AB) and "defective" (A_2B_3) structures in AIII- BVI systems. Part 1. Structural uniqueness and properties of bulk samples and films. Review. *Condensed Matter and Interphases*. 2024;26(4): 646–665. https://doi.org/10.17308/kcmf.2024.26/12398

Для цитирования: Завражнов А. Ю., Брежнев Н. Ю., Некрылов И. Н., Косяков А. В., Кострюков В. Ф. Фазы со слоистыми (AB) и «дефектными» (A_2B_3) структурами в системах A^{III} – B^{VI}. Часть 1. Структурное своеобразие и свойства объемных образцов и пленок. Обзор. *Конденсированные среды и межфазные границы*. 2024;26(4): 646–665. https://doi.org/10.17308/kcmf.2024.26/12398

✉ Alexander Y. Zavrazhnov, e-mail: alzavr08@rambler.ru

1. Introduction

This article is devoted to the description of two large groups of inorganic substances, which are very unusual in terms of their structures and properties, designated as $A^{III}B^{VI}$ compounds. The aim of the study was to summarize, analyze, and, if possible, reconcile data on the structures of $A_1^{III}B_1^{VI}$ monochalcogenides and $A_2^{III}B_3^{VI}$ sesqui-chalcogenides, their hierarchies (parent – daughter structures) and transformations into each other. It should be note that A^{III} tellurides are mentioned here only in general terms, and thallium chalcogenides are not described at all due to the specific nature of the compounds involving heavy *sp*-elements (primarily, the 6th period of the Periodic Table).

Almost all A^{III}–B^{VI} binary systems provide a huge number of different structures (up to two dozen according to [1]). However, the greatest interest of researchers and practitioners is associated with the structural features of solid phases and, consequently, with the specific properties of these substances. Among the huge variety of compositions of compounds, realized for each of these chalcogenide systems, two typical approximate stoichiometries stand out: $A_1^{III}B_1^{VI}$ (monochalcogenides) and $A_2^{III}B_3^{VI}$ (sesqui-chalcogenides). It should be noted that there are large structural differences both *between* two separated groups, and *inside* each of these groups. However, all mono- and sesqui-chalcogenides of Al, Ga, and In have a common unifying feature: all these structures are composed only on (almost) tetrahedral fragments. Such a structure of non-molecular substances is not unusual: as is known that A^IB^{VII}, $A^{II}B^{VI}$, and $A^{III}B^V$ compounds form structures such as sphalerite, wurtzite, and their derivatives, in which each atom is tetrahedrally bound to four neighboring atoms. For the listed compounds, chemical bonds are composed of *s*- and *p-valence* states; they consist of eight electrons for the pair of atoms A and B. However, in A^{III} – B^{VI} systems, pairs of atoms have nine valence electrons. For $A^{III}B^{VI}$ compounds this imbalance in the number of electrons results in structures containing atomic-scale voids that are surrounded by non-separated even-electron orbitals [1]. Let us consider the consequences of this fact for the formation of a variety of structures of the $A_1^{III}B_1^{VI}$ and $A_2^{III}B_3^{VI}$ types, starting with the last group (i.e., with the sesqui-chalcogenides).

2. $A_2^{III}B_3^{VI}$ compounds: general structural features of solids *sesqui*-chalcogenides

The calculation of valence electron concentration (*VEC*) [2, 3] for compounds of stoichiometry, $A_2^{III}B_3^{VI}$ allows sphalerite-like, wurtzite-like, and also derivative structures with CN = 4 (*VEC* = 4.8)* to be formed for these compounds.

Indeed, compounds with such a structure are characteristic of sesqui-chalcogenides of aluminum, gallium, and indium. However, the peculiarities of the above-mentioned electronic imbalance lead to the fact that the $A_2^{III}B_3^{VI}$ phases stand out from other solid substances by containing *stoichiometric vacancies* as structural units (Fig. 1).

* The VEC value is calculated as $VEC = \frac{n_{\bar{e}(A)}n_A + n_{\bar{e}(B)}n_B}{n_A + n_B}$, , where n_A and n_B are the number of atoms A^{III} and B^{VI} in the formula unit of the compound, and $n_{\bar{e}(A)}$ and $n_{\bar{e}(B)}$ are the total number of *s*- and *p*-valence electrons supplied by single atoms of A^{III} and B^{VI} respectively.

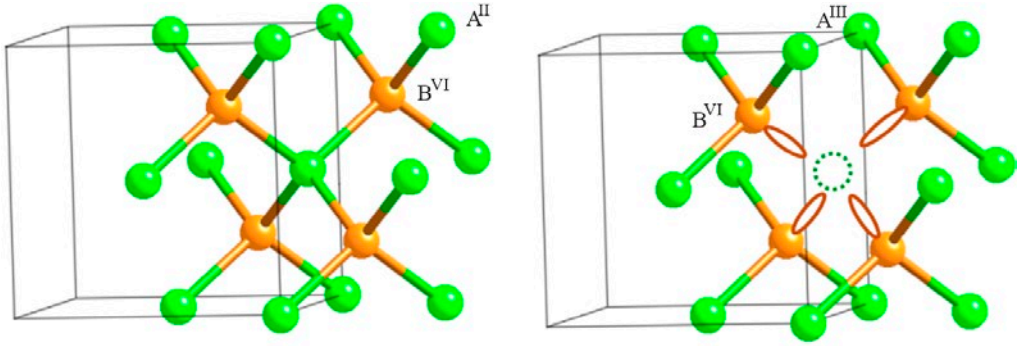

Fig. 1. A fragment of the ideal zinc-blende (sphalerite) structure (left) and a fragment of the sphalerite-like "defective" chalcogenide structure with a stoichiometric vacancy (right). The circle in the form of a dotted line is a stoichiometric vacancy, the ellipses stand for the lone electron pairs of chalcogen atoms directed toward the vacancy

The stoichiometric vacancies occur when disorder takes place in any sublattice (or several at once), arising due to the discrepancy between the stoichiometry and the structural type. As a result, the filling of certain positions in the sublattice by atoms is incomplete, and the unfilled positions are called *stoichiometric vacancies*. Their concentration can be enormous – up to tens of mol. % [2, 4] (p. 105). For the discussed chalcogenides it is about 33 mol. %. This value follows from the fact that the wurtzite or sphalerite-like structure implies a ratio of the number of A atoms to the number of B atoms of 1:1. However, the requirement of 2:3 stoichiometry forces $^1/_3$ of the positions in the cation sublattice to be vacant. Thus, a more appropriate notation for these compounds corresponds to the formula $A^{III}_{\frac{2}{3}}(v_A)_{\frac{1}{3}}B^{VI}$.

If we consider the chemical bond in these compounds to be a covalent pair-electron bond, then the appearance of stoichiometric vacancies can be explained by the fact that chalcogen atoms can form a bond with only three atoms of the cation-forming agent A^{III}, and instead of the fourth bond, such an atom has an orbital with an unshared electron pair, for which there is no suitable vacant orbital. In this case, the A^{III} atoms have all four bonds with chalcogen atoms in the direction of the tetrahedron vertices. It should be noted that such a consideration is not entirely applicable to *indium sulfides*, for which the contribution of the ionic component of the chemical bond is higher.

It should be emphasized that stoichiometric vacancies are structural elements and for this reason, they cannot be fully associated with classical point defects, such as thermal vacancies. Nevertheless, the term "*defective structures*" is used in the literature; the structures of "defective" sphalerite ("defective" wurtzite, "defective" spinel) are also discussed. In some cases, stoichiometric vacancies can order with the formation of a number of their own individual phases of close stoichiometry with a slight distortion of sphalerite-like or wurtzite-like structures.

The terms highlighted here in italics were first introduced in Russian-language scientific literature in 1954 after the studies of N. A. Goryunova [2], [5] and B. F. Ormont [4], and later were developed in the research of the scientific groups of L. S. Palatnik and V. M. Koshkin [6–11]. In the English and French literature, the consideration of special types of vacancies and "defective" structures began in 1949 in studies of Hahn and Klinger [12] and was taken up by Suchet [13].

The discussed compounds allow for obtaining promising materials with the most unusual and diverse characteristics, of which we will consider the most specific ones. First of all, we note that the low coordination numbers and the position of the phase-forming elements in the Periodic Table imply the presence of semiconductor properties for all $A^{III}_2B^{VI}_3$. Moreover, stoichiometric vacancies allow these properties to be maintained practically unchanged even with high concentrations of impurities [14] and with high levels of radiation [8]. Filling of stoichiometric vacancies with atoms of *d*-elements allows isolating these atoms from each other. As a result, for example, in the case of chromium-doped Ga_2Se_3, high ferromagnetic characteristics are already found at room temperature [15]. Lithium atoms can fill these internal voids in $(In_xGa_{1-x})_2Se_3$ nanowires, which is used to create new types of ordered vacancy/lithium atom superlattices and thus obtain lithium-ion storage devices, photovoltaic materials, and phase memory devices [16]. By ideology, the incorporation of lithium atoms is similar to the intercalation of a layered material; however, in the considered sesqui-chalcogenides, the lithium atoms are located on spirals, not on planes. Indium sesqui-chalcogenides, which have a layered structure were demonstrated to be a very promising as photocatalysts for light-induced water splitting [17].

Initial interest in $A^{III}_2B^{VI}_3$ materials, in particular to Ga_2Se_3, arose during the search for ways to create $A^{II}B^{VI}$ heterostructures on $A^{III}B^{V}$ based on the idea of using defective "diamond-like" structures as interlayers. The latter had to match the identically symmetrically oriented single-crystal surfaces of substances with noticeably different lattice parameters. However, this interest quickly faded for a long time, since it was discovered that the impairment of interphase boundaries during the initial stages of the formation of ZnSe-on-GaAs type heterostructures is a serious obstacle [18, 19]. It was later revealed that Ga_2Se_3 on GaAs

itself is a potentially useful material, especially in the form of thin epitaxial film. The Ga_2Se_3 coatings can passivate various oriented surfaces (primarily (001)) of gallium arsenide [20], which has great potential for the use of GaAs taking onto account problems of creating insulating or other functional layers in this important semiconductor. Such layers are needed, first of all, for the creation of optoelectronic devices that use the band gap of gallium arsenide, which is suitable for sunlight [21].

Improvements in molecular beam epitaxy technology in recent years allowed to circumvent the aforementioned problem of interphase boundary impairment when using sesqui-chalcogenides as "interlayer" materials in the formation of $A^{III}B^{V}$ – Si or $A^{II}B^{VI}$ – $A^{III}B^{V}$ type heterostructures [1]. The close correspondence of the lattice parameter of sphalerite-like Ga_2Se_3 to the parameters of Si, GaP, and ZnS substrates facilitate its use in heterostructures. In particular, close lattice matching (0.1%) and minimal interdiffusion at the well-formed Ga_2Se_3/Si interface make such a heterostructure promising for use in electronics. This is due to the fact that the band gap width in epitaxial films of gallium sesqui-chalcogenides is located in a convenient range for visible optoelectronics [22]. In particular, it was proposed to use *n*-alloyed $Ga_2(S_xSe_{1-x})_3$, solid solution deposited on *p*-Si heterojunctions, for solar cells [23]. Among Russian specialists working on obtaining heterostructures using gallium and indium sesqui-chalcogenides as "interlayer" substances or functional coatings when creating heterostructures on $A^{III}B^{V}$ group semiconductors, the scientific group of the authors of the studies [24–27] should be mentioned.

3. "Defective" structure $A_2^{III}B_3^{VI}$ variants: their hierarchy and relationship

Let us consider in more detail the structures of "defective" phases based on wurtzite and sphalerite, paying special attention to the relationship between these structures and the ordering of stoichiometric vacancies. For many compounds in $A_2^{III}B_3^{VI}$ systems, there is a large variety of structures of "defective" various polymorphic phases close to the exact A_2B_3 composition. For some of these compounds, deviations from the ideal composition towards A^{III} component are possible. All $A_2^{III}B_3^{VI}$ structures, except for some modifications of In_2S_3, are composed on almost tetrahedral fragments: A^{III} (Al, Ga, In) atoms, are surrounded by four chalcogen atoms, and the chalcogen atoms, in turn, are surrounded by A^{III} atoms and stoichiometric vacancies. Most of the discussed "defective" structures can be divided into two groups: the so-called "parent" and "daughter" structures. The parent structures are crystals with a fairly high symmetry, these are modifications of the sphalerite or wurtzite type. Structural vacancies in the cation sublattices of these phases are distributed in a disordered manner. Due to the partial or complete ordering of stoichiometric vacancies, such structures can be transformed. In this case, "daughter" structures emerge. For the considered sulfides and selenides, the symmetry of the crystal lattice decreases with ordering. The space group of the crystal also changes. For some $A_2^{III}B_3^{VI}$ modifications, several daughter phases are found (Ga_2S_3, In_2Se_3). This is because the ordering of stoichiometric vacancies can occur in different ways. Daughter modifications with completely ordered structural vacancies are located on the phase diagrams in lower temperature regions, they have narrow homogeneity regions and almost ideally correspond to the A_2B_3 stoichiometry [28–30].

Highly symmetric sphalerite-like structures with disordered stoichiometric vacancies have been found for several metal A^{III} chalcogen systems (γ-Ga_2S_3, α-Ga_2Se_3, α-Ga_2Te_3, α-In_2Te_3). The space group $F\bar{4}3m$ corresponds to such structures, like classical sphalerite ZnS. Due to the deficiency of metal cations, their crystallographic formula is written as $A^{III}(4c)_{2/3}v(4c)_{1/3}B^{VI}(4a)$. The positions of the cation-forming component are 4c ($\bar{4}3m$) (1/4, 1/4, 1/4) occupied by about $^2/_3$. The remaining approximately $^1/_3$ of the positions are not occupied, and these vacant positions are distributed in the cation sublattice in a stochastic manner. Positions 4*a* (43*m*) (0, 0, 0) in the anion sublattice are completely occupied by chalcogen atoms [31] (Fig. 2).

By analogy with zinc sulfide and other substances with "diamond-like" structures, the elementary (almost) tetrahedral "building blocks" of $A_2^{III}B_3^{VI}$ compounds can also fit into wurtzite-type structures (space group $P6_3mc$).

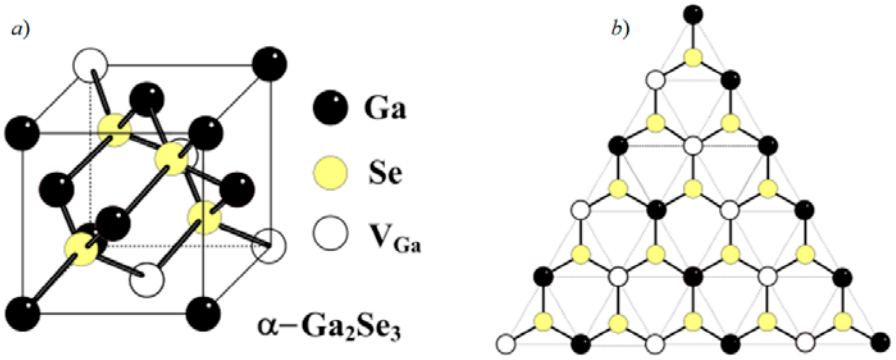

Fig. 2. "Defective" sphalerite-like structure for cubic α-Ga_2Se_3 (a) and the {111} plane in this structure (b) [31].

Like sphalerite-like phases, they contain about $^1/_3$ disordered vacancies in the cation sublattice. The crystal chemical formula of such phases is written as $Me(2b_1)_{2/3}v(2b_1)_{1/3}Ch(2b_2)$, where Wyckoff positions 2*b* (3*m*) (1/3, 2/3, z) are characterized by coordinates: $z_1 = 0$, $z_2 = 3/8$. [12, 30].

Such disordered high-temperature phases can be considered parent phases in relation to "daughter" superstructures. For example, the α-Ga_2S_3 crystal lattice with space group (SG) $P6_1$ was described as a superstructure derived from disordered wurtzite-like β-Ga_2S_3. Similar superstructures are also characteristic of α-Al_2S_3 [32, 33]. In this case, the transformation of the parent phase of "defective" wurtzite into a daughter superstructure occurs with a three-layer ordering of chalcogen vacancies along the [001] axis. According to [28], during such a rearrangement, three crystallographically nonequivalent cationic positions arise, which are completely or partially filled by the A^{III} atoms. Positions of type (1) are almost completely filled: the filling factor is close to 1, and there are practically no vacancies. The cationic positions of type (2) are occupied with a factor of 0.67 and in this respect the occupancy is close to that of all cationic sites in the parent structure of defective "wurtzite". Finally, positions of type (3) are occupied with a factor of 0.35.

This ordering of vacancies requires a change in symmetry from the $P6_3mc$ group to the $P6_1$ subgroup and another choice of the elementary cell with new lattice parameters:

$a_{P6_1} \approx \sqrt{3}a_{P6_3mc}$; $c_{P6_1} \approx 3c_{P6_3mc}$ (Fig. 3). It is important to emphasize that in the resulting daughter structures, each cation position continues to be filled stochastically and, in this sense, we can only discuss quasi-ordering of the structure, in contrast to other types of ordering of stoichiometric vacancies. It should be noted that despite the formation of superstructures with SG $P6_1$, the corresponding phases can be stable only at high (> 900 °C) temperatures. In addition, they have noticeable deviations from the ideal stoichiometric composition [34]. According to these properties, daughter phases with this type of ordering are closer to the parent "defective" structures of wurtzite and sphalerite than to other daughter structures with completely ordered stoichiometric vacancies.

Another type of reorganization of stoichiometric vacancies in the wurtzite-like modification $A_2^{III}B_3^{VI}$ leads to the formation of the second type of daughter phases. In this case, the ordering of vacancies occurs along the vector

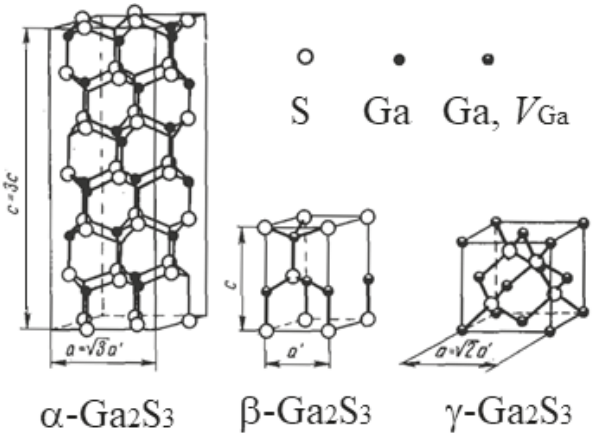

Fig. 3. Structures of some gallium sesquisulfide modifications (present on the phase diagram at high-temperatures, T > 878 °C). From left to right: superstructure of the $P6_1$ type, wurtzite-type defect and sphalerite-type defect structure [28]

[110] of the wurtzite parent lattice and leads to the formation of a monoclinic lattice (space group *Cc*). This structure can already be called ordered due to the presence of entire rows of vacancies in the gallium sublattice (Fig. 4) [31]. The formation of such monoclinic modifications occurs in Ga–S systems (α′-Ga_2S_3), Al – Se (α-Al_2Se_3), as well as in telluride systems. In this case, the ordering also leads to a reduction in symmetry, to a *Cc* subgroup of $P6_3mc$ group and the formation of two cationic and three anionic sublattices of the 4*a* (1) *xyz* family.

The variants for ordering stoichiometric vacancies in wurtzite-like structures do not end there. Several variants of the formation of daughter phases are realized for *indium* sesqui-selenide.

Parental wurtzite-like modification for In_2Se_3, described in [35], is most likely always metastable. Among the phases that can be represented on the *T*-*x*-diagram of the In – Se system, the high-temperature δ-In_2Se_3 structure is closest to this (SG $P6_3mc$). Despite the complete correspondence of this SG to the wurtzite crystal lattice, δ-In_2Se_3, is a superstructure and does not belong to the "true" structural type of wurtzite, since for the latter the ratio of the lattice parameters (*c* to *a*) should be equal to ~1.6 [36]. In our studies, we obtained the following values: *a* = 4.025(1) Å, *c* = 19.265(1) Å [37], which are comparable with the results of [38]: *a* = 4.00 Å, *c* = 6.41 Å. These data indicate a multiple (~3 times) increase in the parameter *c* (4.025×1.6×3 = 19.32 Å) compared to the idealized (by parameter *a*) parent wurtzite structure. The latter may be evidence of the ordering of vacancies, which *in this case* occurs *without a change* of the space group.

The lower temperature modification in comparison with δ-In_2Se_3 is g-In_2Se_3 and it is typical for a $A_2^{III}B_3^{VI}$ semiconductor compound structure with ordered stoichiometric vacancies. According to our research data, the γ-In_2Se_3 polymorphic modification has a hexagonal structure with a space group of $P6_1$ ($P6_5$), (*a* = 7.133 Å, *c* = 19.58 Å) [37]. This is consistent with the results of other researchers [38, 39] – including those who used transmission electron microscopy methods [40, 41]. In [42] it was shown that in the γ-In_2Se_3 phase, structural vacancies are aligned along one of the screw axes, and the proportion of vacancies in the cation sublattice, as in most other $A_2^{III}B_3^{VI}$"defective" semiconductors, is ~ $^1/_3$ of the number of cationic positions. The "defective" crystal structure of γ-In_2Se_3 is shown in Figs. 5 and Fig. 6d.

There are also other modifications for indium sesqui-selenides and sesqui-sulfides which taking into account the definition given at the beginning of this review are no longer entirely correctly classified as "defective" structures with stoichiometric vacancies. In these phases, the ordering of vacancies leads to their grouping into separate planes. As a result, the chemical bonds between the layers

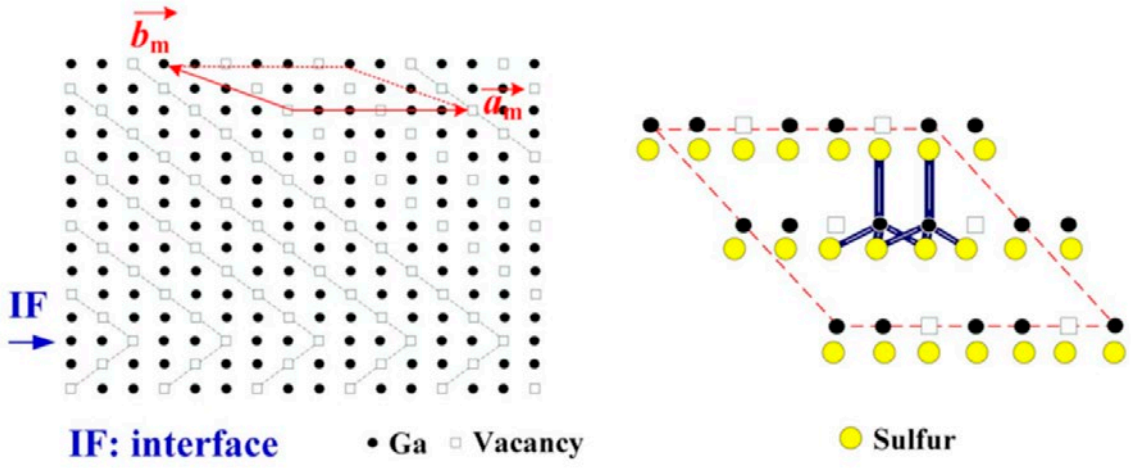

Fig. 4. Fragment of the monoclinic a-Ga_2S_3 structure with an image of stoichiometric vacancies in the Ga-sublattice. The right part of the figure shows the coordination scheme of gallium atoms with an image of chemical bonds close to sp^3-hybrid [31]

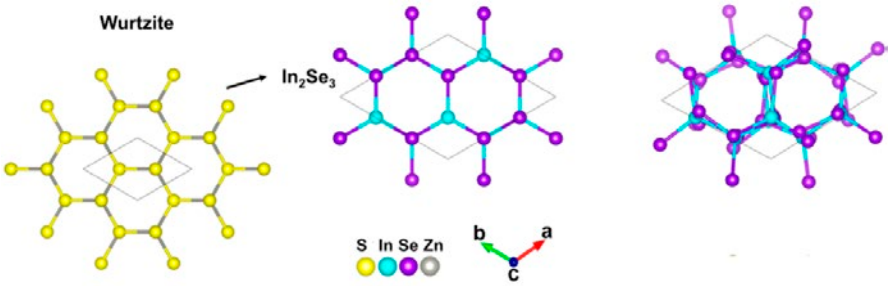

Fig. 5. Relationship between the wurtzite structure (left) with the wurtzite-like idealized structure of In_2Se_3 (center) and the real structure of γ-In_2Se_3 (right)

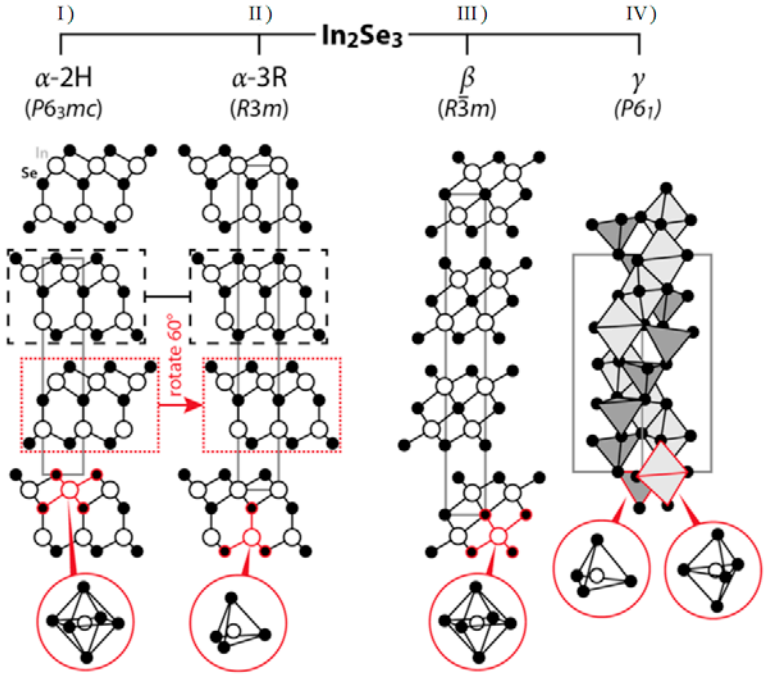

Fig. 6. Structures of In_2Se_3: 2H-α-In_2Se_3 (I), 3R-α-In_2Se_3 (II), β-In_2Se_3 (III) и γ-In_2Se_3 (IV)

are broken and the resulting structures turn out to be typically *layered* and similar in properties to $A^{III}_1B^{VI}_1$ *mono*chalcogenides. In particular, such modifications enter into intercalation reactions, they can easily be exfoliated (splitting into the thinnest layers), etc. In some studies, for example, in [1, 43], the structures under consideration continue to be classified as "defect-vacancy" structures, taking into account that individual layers are formed precisely by the ordering of vacancies. However, it should be noted that with this approach the definitions *compounds with stoichiometric vacancies* and "*defective*" *phases* will require correction.

The following relatively low-temperature modifications are classified as *layered* forms of indium sesqui-selenide: 2H-α-In_2Se_3, 3R-α-In_2Se_3 and β-In_2Se_3 [44]. The lowest temperature 2H-α-In_2Se_3 form (exists when t < –125 °C) belongs to the space group $P6_3mc$ with cell parameters a = 4.025 Å, c = 19.235 Å [45]. The 3R-α-In_2Se_3 trigonal modification is stable at room temperature and belongs to the space group $R3m$ with the parameters a =4.052 Å, c = 28.765 Å. Structures of both a-phases are shown in Fig. 6A and Fig. 6b. For the 3R polytype, the characteristic sequence of layers is ABCABC, for 2H it is ABAB. In both cases, individual layers are composed of five-layer stacks in which Se–In–Se–In–Se chains can be traced.

The β-In_2Se_3 "medium temperature" phase is characterized by a space group $R\bar{3}m$ with lattice parameters a = 4.05 Å, c = 29.41 Å. The main difference of this phase (Fig. 6c) from 3R-α-In_2Se_3

in that selenium atoms occupy octahedral positions instead of tetrahedral ones for α-In_2Se_3 (if we consider these structures as formed by indium atoms with dense hexagonal packing).

It should also be noted that the formation of buffer layers on diamond-like (cubic $F\bar{4}3m$ or hexagonal $P6_3mc$) structures can lead to the formation of coatings with both a layered structure (in the case of In_2Se_3), as well as non-layered films with "defective" structures of sphalerite or wurtzite (in the case of Ga_2Se_3, Fig. 7) [43], due to the different organization of stoichiometric vacancies.

Finally, another existing type of sesqui-chalcogenide with stoichiometric vacancies is fundamentally different from all the above types, since it corresponds to a different ideal stoichiometry: A_3B_4 instead of A_2B_3. These include structures with a high proportion of ionic bonds, which have a spinel crystal lattice [46]. The most famous, and probably the only representative of this type among the chalcogenides of group III metals, are the $In_{3-x}S_4$ phases.

In most literary sources this phase is written as α-In_2S_3, which, in our opinion, is not entirely

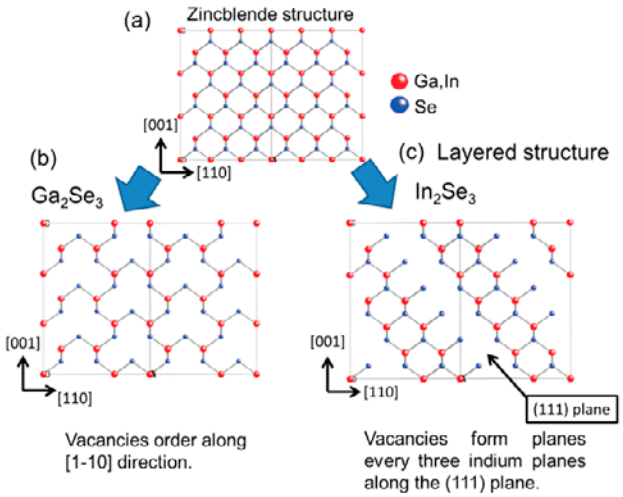

Fig. 7. Mutual relationships between certain surfaces of the following structures: a) – sphalerite, b) – "defective" gallium sesquiselenide with ordering of vacancies (without formation of a layered structure and with) and c) – "defective" indium sesquiselenide (with formation of a layered structure) [43]. Left: vacancies are ordered along the [1$\bar{1}$0]; direction; right: stoichiometric vacancies form planes, grouping every three planes formed by indium atoms, which are located along the (1 1 1) plane

correct. The In_2S_3 formula is explained by the fact that, according to stoichiometry, this phase is closer to sesqui-sulfide (58.5 – 59.5 mol. % S) according to our studies [47, 48]. The $In_{3-x}S_4$ phase (a-In_2S_3) has a *cubic* crystal lattice of inverse spinel (SG $Fd\bar{3}m$, a = 10.724 Å [46, 49–51]), in which there is a deficit of indium atoms compared to the ideal stoichiometry of In_3S_4 (~ 57.1 mol. % S). This modification exists in the "medium temperature" range (according to our data [49] – from 418 to 752 °C, which correlates well with [52]). It is easily hardened and can be isolated at room temperature. According to the latest source, the formula of this compound is most correctly written as $[In_{2/3}(v)_{1/3}]^{tetr}[In_2]^{oct}S_4$, where the symbols "*tetra*" and "*oct*" denote positions in the tetrahedral and octahedral voids of the spinel packing, the framework of which is formed by sulfur atoms; vacancies are designated by the "v" symbol. The given formula follows from the assumption (approximation) that in classical spinels there are charge states of metal M^{2+} and M^{3+}; in the case of indium, taking into account the peculiarities of its classical chemistry, we should discuss the In^{+1} and In^{+3} states. Then the formula $[In_{2/3}(v)_{1/3}]^{tetr}[In_2]^{oct}S_4$ corresponds to the stoichiometry of $In_{2.67}S_4$ = In_2S_3. If the charge states of In^{+2} are allowed, then the given formula will be close to the typical spinel composition M_3S_4. Experimental data, as we already noted, show an intermediate situation between the two stoichiometries. It should be noted that vacancies in cubic form are distributed stochastically among positions (primarily tetrahedral).

On the contrary, in the low-temperature form β-In_2S_3 there is an ordering of vacancies (Fig. 8), and the structure with a decrease in symmetry turns into a tetragonal one (SG $I4_1/amd$; a = 7.61 Å, c = 32.24 Å). This phase exists on the phase Tx-diagram up to 418 °C and is easily released during annealing of any other modification of indium sesqui-sulfide below the specified temperature [49]. For the two compounds mentioned, the cubic structure $In_{3-x}S_4$ (α-In_2S_3) can be considered maternal, and the ordered β-In_2S_3 structure is a daughter structure.

In conclusion in this review of defective indium sesqui-sulfides, we will consider the third, most high-temperature and controversial modification in terms of structure, which is γ-In_2S_3. According

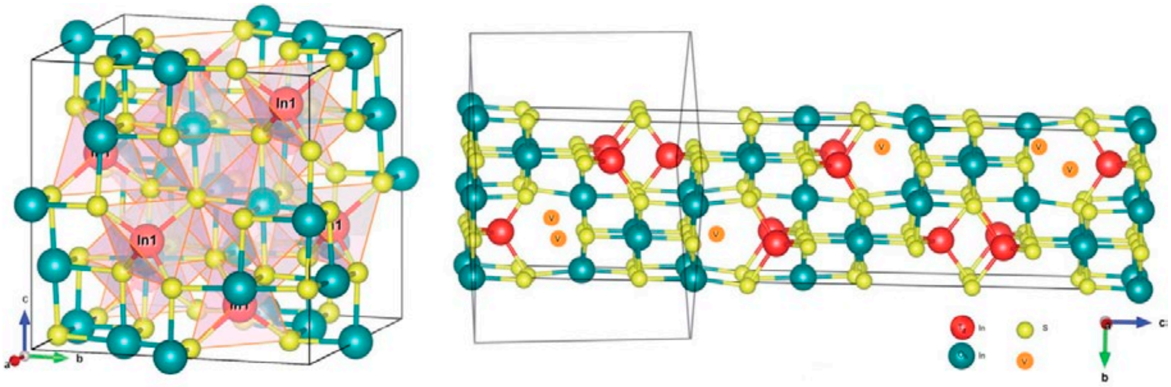

Fig. 8. Structures of In_2S_3: spinel-like, with a more correct formula $In_{3-x}S_4$ (left), tetragonal In_2S_3 (left) [56]

to [52] the structure of this trigonal (SG $R\bar{3}m1$) phase is not spinel-like and is probably close to β-modifications of sesqui-*selenide* indium – i.e., it is layered and formed from a wurtzite "defective" structure due to such an ordering of vacancies that they form separate planes that open separate five-layer packets S–In–S–In–S [53, 54]. This conclusion is not supported by the authors of recent publications [55] and [56], who insist that γ-modifications belongs to the structural type of defective Th_3P_4. In the latter, the cation-forming atoms stochastically occupy only octahedral voids with a filling factor of ~89%. The difficulty of unambiguous interpretation of the structure γ-In_2S_3 is because the pure phase is not quenched, and the authors [56] isolated it by the rapid cooling of a sample deliberately contaminated with vanadium and titanium impurities.

4. $A^{III}_1B^{VI}_1$ compounds: general structural features of solids *mono*chalcogenides

Monochalcogenides typically provide layered structures in which individual four-layer $B^{VI}–A^{III}–A^{III}–B^{VI}$ packets are bound to each other only by weak van der Waals forces (Fig. 9) [1]. The exception is to some extent is α-InS* [49, 57–59].

These compounds are often referred to by technologists as "van der Waals materials." Their ability to exist in isolation as individual B–A–A–B layers opens up prospects for their use in emerging two-dimensional electronics [60].

In $A^{III}B^{VI}$ layered compounds each four-layer stack is composed of two planes containing B^{VI} chalcogen atoms. Layers consisting of such atoms are located on both sides of two adjacent intra-packet planes; in the latter, there are atoms of group III elements bound with each other (and with B^{VI} atoms) (Fig. 9). The basic building block is formed by stacking four hexagonal monoatomic sheets in the sequence B–A–A–B with trigonal prismatic symmetry. Different stacking and/or 180° rotation of these covalently linked layers results in the formation of several polytypes, some of which exhibit inversion symmetry. This fact indicates that, for example, depending on the presence or absence of such symmetry, the linear and nonlinear

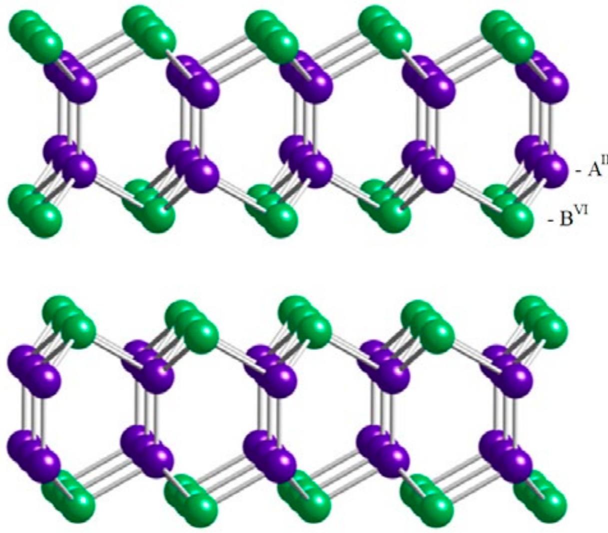

Fig. 9. Fragment of the layered monochalcogenide $A^{III}B^{VI}$ – structure [1]

* At the same time, there is no reliable information about the bulk structures of aluminium monochalcogenides, although the structure of epitaxial films of nanoscale thickness turned out to be close to the structures of other typical layered monochalcogenides. There is also no reliable structural data on the high-temperature form of β-InS, which exists in very narrow (slightly more than 10 °C) temperature range.

optical properties of layered $A^{III}B^{VI}$ will depend on the resulting polytype [61].

The B–A–A–B sequence in quasi-two-dimensional $A^{III}B^{VI}$ layered semiconductors leads to an unusual combination of different types of chemical bonds, which in turn provides non-trivial electronic states [1]. Interlayer bonding is achieved through weak van der Waals interactions with strong intralayer interactions. The covalent homodesmic bond "cation–cation" is non-polar, while the heterodesmic bond "cation–anion" has a partially ionic character [59]. In all three substances, the valence electrons are strongly localized around the B^{VI} atoms, and two A^{III} atoms are bound almost exclusively by a s-bond formed by *s*-electrons. With an increase in the proportion of ionicity from GaSe (0.66) to GaS (0.74) and to InSe (0.80), the ionic nature of the A^{III}–B^{VI} bond obviously increases and the electron density shifts towards to B^{VI} atoms. Moreover, if the gallium atom is replaced by indium or selenium is replaced by sulfur, then the atomic *s*-states of atom A^{III} become less separated in energy from the *p*-states of B^{VI}. The latter is reflected in the delocalization of the bond charge A^{III}-A^{III} and a weakening of the central bond with increasing bond length. A further increase in ionicity leads to the fact that the low-temperature modification a-InS is structurally unique among $A^{III}_1B^{VI}_1$ compounds, since it ceases to be a fully layered 2D structure. In α-InS, it is still possible to distinguish individual S–In–In–S packets, but they are no longer isolated from each other: with a long and weak In–In bond, one packet creeps and wedges into another. As a result, sulfur atoms belonging to one package bond with indium atoms from the neighboring package. In this way, a 3D orthorhombic structure is formed (Fig. 10), in which there are no layers bound only by van der Waals forces [59].

An increase in the size of chalcogen atoms also leads to a change in structure. Thus, layered 2D-structure consisting of loosely coupled four-layer stacks is retained during the GaS → GaSe → GaTe transition. However, for α-GaTe layers, instead of being flat become corrugated (Fig. 11), and the structure changes from hexagonal (2H and 4H polytypes) or rhombohedral (3R polytypes) to monoclinic [62, 63]. At the same time, there is always a metastable modification b-GaTe with a package arrangement identical to gallium monoselenide (Fig. 9) [63].

5. Intercalation reactions in $A^{III}_1B^{VI}_1$ layered crystals (and α- and β-In_2Se_3)

Taking into account the described structural features of aluminum, gallium, and indium monochalcogenides, these substances should be characterized by intercalation reactions i.e.

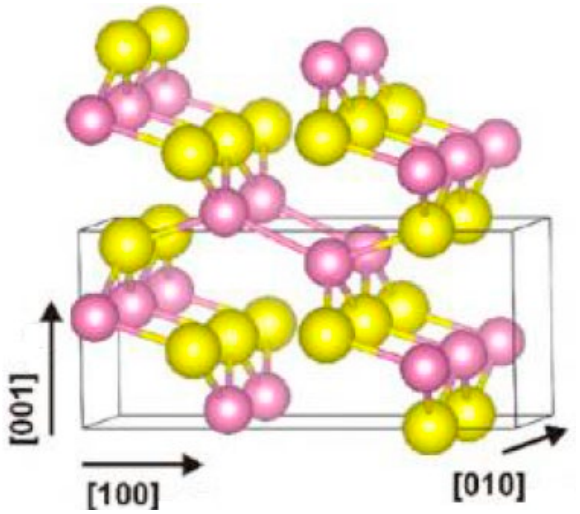

Fig. 10. Fragment of α-InS structure (orthorhombic LT-modification)

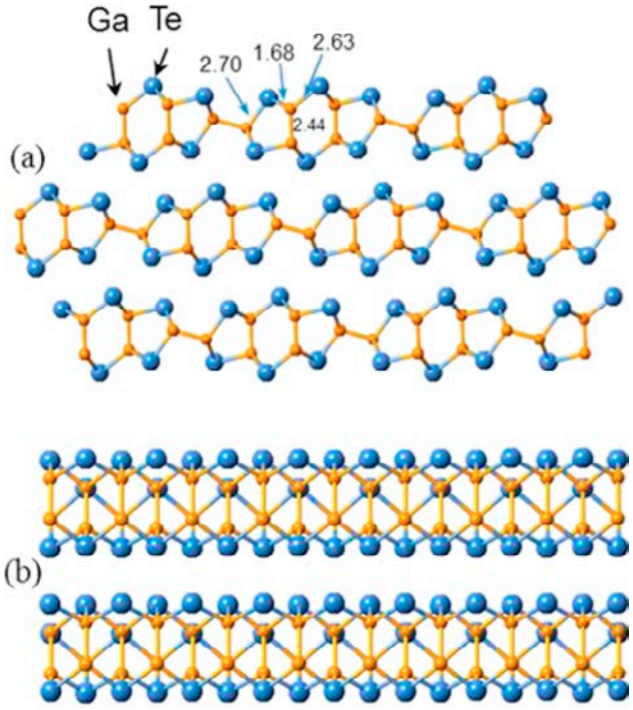

Fig. 11. Frontal (a) and side view (b) of the structure and the layers arrangement in the α-GaTe 3D-structure

interactions associated with the entry of atoms (molecules, ions) into the space between weakly bound 2D layers or 1D chains, as well as the introduction of atoms into atomic-level channels. It should be remembered that the ordering of stoichiometric vacancies is characteristic of $A_2^{III}B_3^{VI}$ sesqui-chalcogenides and can also lead to the formation of structures such as low and medium temperature forms of indium selenide (α-2H- and β-In_2Se_3) with very weakly connected individual layers. As a result, both for the last phase and for almost all $A_1^{III}B_1^{VI}$ monochalcogenides, there are numerous publications on intercalation reactions and on the production of interlayer insertion products – intercalates (reviews [64, 65]).

The peak of interest in such objects and attempts at their practical use occurred in the 90s and 2000s at the turn of the 20th and 21st centuries. In particular, the authors of [64] reported on a project to reduce background radiation in the territory of the Chernobyl Nuclear Power Plant by applying monocrystalline GaSe plates to the internal walls of the damaged power unit and other structures: it was assumed that atoms of iodine isotopes and other radioactive elements in the air would spontaneously be introduced into the layered structure of gallium monoselenide. However, numerous difficulties in the study and the reproducibility of obtaining intercalates of $A^{III}B^{VI}$ compounds led to a decline in interest in these objects.

The guest (implanted) particles included both the smallest particles, individual atoms (ions) of alkali, alkaline earth, rare earth elements, and some other elements, as well as whole molecules with predominantly expressed basic (according to Lewis) properties, from ammonia to pyridine or anthracene, as well as relatively large ions that enter the structure during the processing of A^{III} monochalcogenides by solutions and melts of nitrites and nitrates [64, 65]. Most often, direct interaction of the crystal with the substance-source of guest atoms (incorporation upon contact with the gas or liquid phase) or electrochemical reactions involving solutions (melts) in which monochalcogenides were electrodes were used for the synthesis of such intercalates. One of the authors of this study investigated the interlayer incorporation that occurs during the treatment of single-crystal GaSe and InSe with concentrated nitric acid, solutions of some nitrates, nitrogen tetroxide [66, 67], as well as pyridine and anthracene [68].

It should be noted that we were unable to carry out any intercalation reactions involving gallium monosulphide. In the literature, data on this issue are also extremely scarce. In existing studies, for example in [69], the exfoliation of GaS via the stage of formation of an intermediate intercalated compound was described. However, this stage preceding exfoliation is not analyzed in any way. The reason for the difficulties with interlayer implantation in GaS is probably the too small size of the sulfur atoms lining the interlayer spaces between the packets [1].

Intercalation is most clearly manifested during diffraction structural studies. It is recorded by the shift towards small angles of such reflexes, which are associated with an increase in the distances between planes connected by Van der Waals forces. In some cases, the increase in distances in the direction perpendicular to the layers is observed even visually as an anisotropic "swelling" of the crystal during its intercalation [67–70]. However, small-sized embedded atoms (especially of those *d*-elements as Cu or Pd) seem to pull together the adjacent packages and then the corresponding interplanar distances hardly change or even decrease [71].

In our studies [72, 73] the possibility of autointercalation (with selenium) is considered as being the reason for the significant expansion and displacement (up to 0.6–0.8 mol. %) of the homogeneity region of gallium monoselenide towards selenium in a relatively narrow temperature range close to the congruent melting temperature of GaSe. The hypothesis about the relationship between the specific type of homogeneity region of this phase and autointercalation, the interlayer introduction of atoms of one of the phase-forming components, is described in more detail when examining the phase diagram of the Ga–Se system.

In publications on the study of intercalates, noticeable differences in the electrophysical, optical, catalytic, and other properties of intercalated semiconductors compared to the original substances are almost always noted. In a number of cases, these properties are described as very promising for materials

science. In particular, it was shown in [67] that the introduction of palladium(II) nitrate (from aqueous solutions) into GaSe followed by a reduction of the intercalated product led to the production of a material with pronounced catalytic properties typical for matrices activated by palladium.

However, there are several unresolved problems to this day, which have led to a hopefully temporary decrease of interest in the interlayer introduction into of $A^{III}B^{VI}$ compounds into bulk crystals. In our opinion, the main unresolved problem is the uneven progress of introduction. It is often unclear what part of the crystal and what areas within it were affected by interlayer incorporation. It is well known that guest particles often do not fill every van der Waals gap, they are incorporated through a certain *n*-number of layers (in this case, the formation of an intercalate of the *n*-stage is discussed). However, for the considered structures, a different case most likely occurs: intercalation occurs stochastically, and the number of layers affected by the incorporation may not exceed several percent of their total number (as shown, for example, in the course of studies using a zero-manometer in [68]). In addition, in the bulk $A^{III}B^{VI}$ crystal, probably, there are adjacent layers with a large number of defects (superstoichiometric atoms, layers of another polytype (another phase) with the thickness of several atomic layers, etc.). It is assumed that intercalation occurs *only* into such interlayer regions without affecting the bulk of the crystal. At the same time, in almost all studies on this topic (for example, those described in the review paper [64]), neither the composition of the obtained substance nor the uniformity of the distribution of the guest impurity throughout the volume of the crystal is reported.

The next problem is that intercalation is often destructive: guest molecules or ions actively interact with the substance into which they have been incorporated, changing themselves and altering the structure of the host. In particular, the analysis of the product of GaSe treatment with nitric acid, carried out by one of the authors of this study, revealed Ga–OH, Se–OH, Se=O fragments associated with the initial selenide matrix [66, 67]. Probably, the same destructive processes occur when GaSe (InSe) is treated with nitrite and nitrate melts [64]. These reactions show an analogy with the oxidative incorporation of acids such as $HClO_3$, HNO_3, $HMnO_4$, etc., into graphite, when the incorporated substance partially oxidizes the layers "from the inside", producing carboxyl, ketone, hydroxyl and other groups covalently bonded to the damaged graphite layers ([66, 74]. Fig. 12).

Unfortunately, the possibility of "internal corrosion" of an intercalated layered crystal is often not considered at all, although it can lead to both irreproducibility and degradation of the material properties. Local changes at the atomic level are especially possible for *electrolytic* method of incorporation since the layered structure can include solvent molecules and other foreign impurities active in terms of further oxidation-reduction interactions.

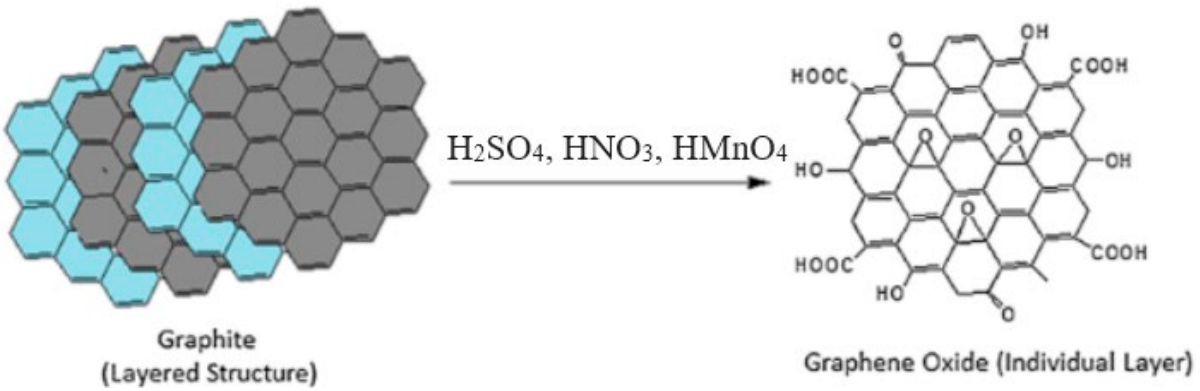

Fig. 12. Changes in the structure of graphite when exposed to acidic oxidizers (HNO_3, $HClO_3$, $HMnO_4$, etc. in strongly acidic solutions) with the formation of damaged graphene layers with hydroxyl, carboxyl, ketone and epoxy-like groups [74]

Despite the slowdown in progress in the ideas and application of intercalation of $A^{III}B^{VI}$ for the design of promising semiconductor and nonlinear optical materials, attempts are currently ongoing to use interlayer incorporation to create new chemical current sources (CCS) [75] (p. 136), combining nanolayers of different layered substances (for example, In_2Se_3 and MoS_2), obtained after intercalation (with lithium) and subsequent spontaneous cleavage (exfoliation) of the intercalate into graphene-like nanoplatelets [76]. In addition, the method of obtaining roquesite-like materials (of Cu(Ag) Ga(In)Se_2 type) when intercalating the matrix of monochalcogenide A^{III} with copper with subsequent stimulated (for example, thermally) restructuring of the intercalate seems to be original [71].

6. Nanostructures based on $A^{III}B^{VI}$ monochalcogenides

The similarity of monochalcogenides to graphite and similar layered substances such as black phosphorus does not end with intercalation reactions. The $A^{III}B^{VI}$ monochalcogenides and adjacent layered modifications of sesqui-chalcogenide In_2Se_3 can exist in the form of nanolayer graphene-like thin-layer fragments, forming nanoribbons and nanotubes (tubulenes).

Nanolayered graphene-like monochalcogenides of gallium and indium

The unique properties of nanolayered (ideally single-layered) layered substances make them promising for a wide range of applications [77–79]. Containing a small number of layers, (nano)monocrystalline gallium and indium chalcogenides are obtained in different ways, among which the simplest option consists of breaking the monocrystal into layers for example, by stretching a polymer tape such as Scotch tape glued on both sides in opposite directions, predominates. The breaking procedure is repeated many times until the layer remaining on the tape becomes dark grey (after going through stages of obtaining intensely colored due to interference thicker layers). As a result, after removing the adhesive organic polymer, fragments of monochalcogenide layers up to 300 nm thick are obtained [60].

Among other methods, a variant where the splitting (exfoliation) of a bulk single crystal into individual plates is carried out during the electrolysis of a solution using a single crystal of a layered substance as a cathode draws attention. Solutions of alkali metal salts (mainly lithium; usually in the form of $LiClO_4$ [80]) are usually used as electrolytes in water or in ionic organic solvents. Intercalated chalcogenide is obtained by this method. Then a salt of an organic nitrogenous base (most often tetrabutylammonium salt) is added to the solution and electrolysis continues. The huge cations entering between the layers finally break these layers, which are then released in the form of a suspension [81]. It should be noted that when electrolytic exfoliation was carried out, the fact of intermediate formation of intercalate was not always proven. Moreover, the indicated method allowed to obtain nanolayer fragments of even indium monosulphide (a-InS), in which individual layers are bound by a chemical (ionic-covalent) bond [82].

Among the properties of a suspension of individual nano-sized fragments of phases of different layered crystals, the ability of these fragments to self-assemble into a kind of three-dimensional heterostructure should be highlighted. This includes, in particular, a heterostructure "self-assembled" from individual alternating nanolayer fragments of indium selenide and molybdenum disulfide [75].

Among the chalcogenide "true" 2D structures, monolayer gallium monosulphide (*mono*-2D-GaS) was recently investigated and studied [79, 83]. Materials based on *mono*-2D-GaS have proven promising for use in hydrogen evolution reactions [84], as well as in the creation of promising lithium-ion batteries [85], nonlinear optics materials [86], photodetectors [87], and gas sensors [88]. The tetra atomic in thickness (single S–Ga–Ga–S packet) monolayer GaS is a semiconductor with a wide band gap of ~3.33 eV, which is ~0.8 eV larger than for a bulk GaS single crystal [89].

Nanotubes (tubulenes) from indium and gallium monochalcogenides layers

Nanotubes, the closest analogues of carbon nanotubes, are the most studied for gallium monoselenide. The first studies on such

nanotubes appeared, probably, in the 90s. The first publications reported only the results of quantum chemical calculations confirming the possibility of the appearance of such structures. In particular, in [90] an image of a predicted fragment of such a GaSe nanotube is given (Fig. 13). Now such tubulenes have been obtained not only for GaSe, but also for GaS. For the synthesis of both sulfide and selenide nanotubes, a long-term (72 h) interaction of gallium acetylacetonate with chalcogen in an organic solvent (dodecylamine, hexadecylamine) at elevated temperature (200 °C) was used [91].

In [92], spontaneous twisting of some nanolayer fragments of InSe obtained during ultrasonic exfoliation of bulk indium monoselenide samples in isopropanol was noted. The resulting nanotubes had a diameter of less than 1 nm.

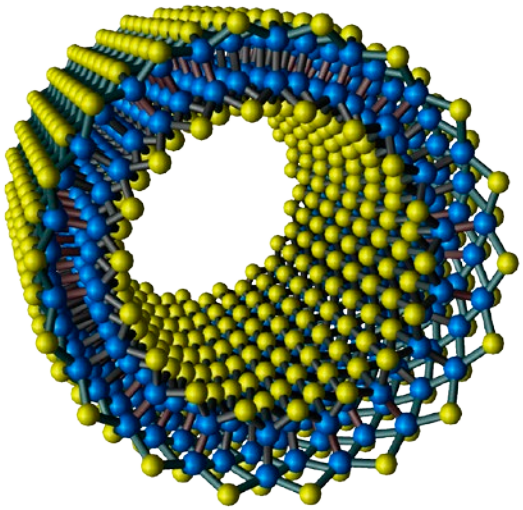

Fig. 13. GaSe nanotube Structure [90]

7. Some aspects of application of single-crystal layered monochalcogenides $A^{III}B^{VI}$ as new promising materials for nonlinear optics

Layered bulk $A^{III}B^{VI}$ crystals exhibit strong optical and electrical anisotropy [93, 94] and high nonlinear optical coefficients in the infrared range [95], which makes them candidates for materials for the generation of second-harmonic radiation (primarily IR lasers) [96–100]. This interest led to extensive work in the 1970s and 1980s on the production of GaSe and InSe bulk single crystals. Many optical and electrical properties of these substances have also been studied in detail [101]. Among the gallium monochalcogenides, gallium monoselenide has the greatest practical significance. Air-stable layered red-ruby single crystals of gallium monoselenide are somewhat similar to colored mica, but heavier (density of 5.03 g/cm^3) and softer (microhardness of 30 kg/mm^2) [14].

Gallium monoselenide is a high-resistance semiconductor with low electron and hole concentrations and low carrier mobility values. Due to low carrier concentrations and low mobility values, this material was long considered an unpromising indirect-gap *p*-type, regardless of the method of production and doping (the transition energy between the valence band and the conduction band is 2.03 eV with a difference in energy between the direct and indirect transitions in GaSe of 0.025 eV) [101].

However, in the last decade, the attitude towards GaSe has changed fundamentally, which is associated with its use in nonlinear optics [78, 98, 101–103]. Currently, various optical systems are being developed on gallium monoselenide, which are used for:

- the generation of second-harmonic radiation of CO_2 laser or similar types of coherent radiation generators (doubling the output frequency when exciting the crystal with short-pulse radiation in the wavelength range from 6.3 to 12 μm); the output signal is stable for many hours with conversion efficiency up to 36%;
- the conversion of frequency of radiation of CO_2 laser into the high-energy region up to the visible region or near IR range (the so-called "up-conversion" [102]);
- the generation of sum frequencies in the mid-IR region;
- the generation of difference frequencies in the mid-IR region from 5.5 to 18 μm;
- creation of radiation-resistant photodiodes designed for the visible and near IR spectral range in the spectral range of 0.6–1.1 μm (for night vision devices) [104];
- the creation of solid-state laser systems based on parametric generation of light using pumping of various types of lasers (for example, those based on Nd-doped yttrium aluminum garnet). A special case of the latter systems are

devices for generating terahertz frequencies with ν = 10^{11}–10^{12} Hz) [98,105].

We will discuss the last possibility of practical use of materials based on GaSe single crystals in more detail. It is known that electromagnetic waves have a length l = 100-1000 μm (these correspond to the vibration frequencies ν = $3{\cdot}10^{12}$ 10^{11} Hz), and occupy an intermediate region between the long-wave infrared and ultra-high-frequency radio ranges. These waves, called terahertz waves, are of considerable interest for a variety of applications, including biology, medicine, and archaeology. Similarly to X-rays, terahertz radiation has high penetrating power, but, unlike the former, does not pose a danger to living organisms or ancient objects. However, until recently, the terahertz range remains one of the technically poorly equipped parts of the spectrum.

The situation has only fundamentally changed in the last decade with the development of various materials, including those constructed from In and Ga monochalcogenides [1], [101, 105, 106]. In particular, a compact terahertz source capable of producing radiation in the range between 56.8 and 1618 microns (from 0.18 to 5.27 THz) was created based on GaSe crystals [107, 108]. In [108] it was noted that the key advantages of such a DFG are an extremely wide tuning range, high stability, small size, and high peak power. Moreover, according to [107], in terms of the accuracy of tuning the wave range, no other terahertz sources can compete with a GaSe-based device.

The production of other layered gallium monochalcogenides as materials for nonlinear optics is also under development. For example, gallium monosulphide (lemon-yellow, mica-like crystals; indirect-gap semiconductor of *n*-type with E_z =2.5 eV) has good photoconductivity in the ultraviolet part of the spectrum [86, 109]. The indium monosulphide (dark brown crystals; semiconductor of *n*-type with several approximate levels; E_z = 1.9 eV) [110] and gallium monotelluride [111, 112] are also promising as photoconductive materials.

8. Conclusions

Unfortunately, the practical use of $A_2^{III}B_3^{VI}$ chalcogenides with various "defective" structures depends, first, on the problem of reproducible synthesis of each of the many modifications considered here. For bulk samples, this problem is primarily because for many binary systems, it has not yet been possible to obtain a consistent idea of the location of the discussed intermediate compounds on the corresponding phase diagrams. In addition to regulating the phase composition, i.e. the structural affiliation of the resulting compound, a problem of the next level is added, associated with the need to regulate the composition within the homogeneity region of a specific phase for a finer "tuning" of the properties of the resulting substance. The latter task is also relevant for film coatings that are parts of the formed heterostructures.

In relation to $A_2^{III}B_3^{VI}$ monochalcogenides the regulation of the polytypic affiliation of the obtained layered single crystals is important (which is a special, but more complex case of the problem of regulation of the phase composition). Thus, the question about the relationship between the main characteristics of the device with the non-stoichiometric composition of the crystal and its belonging to a certain polytype has never been raised in any of the cited studies on the use of monoselenide or related layered monochalcogenides for generators of various long-wave radiation. At the same time, in many studies (for example, in [97]) it was noted that it is impossible to obtain reproducible characteristics of the output radiation without high-quality control of the composition of materials. Approaches to these questions will be considered in the second part of our review.

Contribution of the authors

The authors contributed equally to this article.

Conflict of interests

The authors declare that they have no known competing financial interests or personal relationships that could have influenced the work reported in this paper.

References

1. Olmstead M. A., Ohuchi F. S. Group III selenides: controlling dimensionality, structure, and properties using through defects and heteroepitaxial growth. *Journal of Vacuum Science and Technology A: Vacuum, Surfaces, and Films*. 2021;A39: 020801. https://doi.org/10.1116/6.0000598

2. Goryunova N. A. *Complex diamond-like semiconductors**. Moscow: Sovetskoe Radio Publ.; 1968. 268 p. (In Russ.)

3. Parthé E. *Elements of inorganic structural chemistry*. CH-1213: Petit-Lancy, Switzerland; 1996. 230 p.

4. Ormont B. F. *Introduction to physical chemistry and crystal chemistry of semiconductors*[*]: Textbook. V. M. Glazov (ed.). 3rd ed., corrected and enlarged. Moscow: Vysshaya Shkola Publ.; 1982. 528 p. (In Russ.)

5. Goryunova N. A. Some issues of crystal chemistry of compounds with zinc blende structure[*]. *Izvestiya Akademii nauk SSSR. Fizika.* 1957 21(1): 120. (In Russ.)

6. Atroschenko L. V., Zhuze V. P., Koshkin V. M., Ovechkina E. E., Palatnik L. S. The property of chemical inertness of metal impurities in semiconductors with stoichiometric vacancies[*]. *Byulleten' izobretenii i otkrytii SSSR*. 1981;41: 1. (In Russ.)

7. Palatnik L. S., Komnik Yu. F., Koshkin V. M. Crystal chemistry of compounds with tetrahedral coordination of atoms[*]. *Kristallografiya*. 1952;7(4):563–567. (In Russ.)

8. Koshkin V. M., Volovichev I. N., Gurevich Yu. G., Galchinetsky L. P., Rarenko I. M. Materials and devices with a giant radiation resource[*]. *Materials of scintillation technology: Institute of Single Crystals*. 2006: 5–60. (In Russ.)

9. Palatnik L. S., Rogacheva E. I. Equilibrium diagrams and structure of some semiconductor alloys $A_2^IC^{VI}$–$B_2^{III}C_3^{VI}$[*] *Soviet Physics Doklady*. 1967;174(1): 80. (In Russ.)

10. Palatnik L. S., Koshkin V. M., Komnik Yu. F. *Chemical bonding in semiconductors and solids*[*]. Moscow: Nauka i Tekhnika Publ.; 1965. 301 p. (In Russ.)

11. Atroshchenko L. V., Galchinetsky L. V., Koshkin V. M., Palatnik L. S. *Deviations from stoichiometry and solubility of impurities in semiconductors with stoichiometric vacancies. Chemical bonding in semiconductors and thermodynamics*[*]. Minsk: Nauka i Tekhnika Publ.; 1966. 261 p. (In Russ.)

12. Hahn H., Klingler W. Über die Kristallstrukturen von Ga_2S_3, Ga_2Se_3 und Ga_2Te_3. Z. *Zeitschrift für anorganische Chemie*. 1949;259(1-4): 110–119. https://doi.org/10.1002/zaac.19492590111

13. Suchet J. P. *Chimie physique des semiconducteurs*. Dunod, France. 1962. 361 p.

14. Madelung O. III_2–VI_3 compounds. *Semiconductors Data Handbook*. Springer, Berlin. 2004:275–288. https://doi.org/10.1007/978-3-642-18865-7

15. Yitamben E. N., Lovejoy T. C., Pakhomov A. B., Heald S. M., Negusse E. Correlation between morphology, chemical environment, and ferromagnetism in the intrinsic-vacancy dilute magnetic semiconductor Cr-doped Ga_2Se_3/Si(001). *Physical Review B*. 2011;83: 045203. https://doi.org/10.1103/PhysRevB.83.045203

16. Peng H., Zhang X. F., Twesten R. D., Cui Y. Vacancy ordering and lithium insertion in III_2VI_3 nanowires. *Nano Research*. 2009;2: 327-335. https://doi.org/10.1007/s12274-009-9030-y

17. Zhao P., Ma Y., Lv X., Li M., Huang B. Two-dimensional III_2-VI_3 materials: promising photocatalysts for overall water splitting under infrared light spectrum. *Nano Energy*. 2018;51: 533. https://doi.org/10.1016/j.nanoen.2018.07.010

18. Krost A., Richter W., Zahn D. R. T. Chemical reaction at the ZnSe/GaAs interface detected by Raman spectroscopy. *Applied Physics Letters*. 1990;57: 1981. https://doi.org/10.1063/1.104149

19. Wright A. C., Williams J. O. Detection of compound formation at the ZnSe/GaAs interface using high resolution transmission electron microscopy (HRTEM). *Journal of Crystal Growth*. 1991;99: 114. https://doi.org/10.1016/0022-0248(91)90684-W

20. Takatani S., Nakano A., Ogata K., Kikawa T. Structure of chalcogen-stabilized GaAs interface. *MRS Proceedings*. 1992;31: L458. https://doi.org/10.1557/PROC-281-677

21. Guler I., Isik M., Gasanly N. M., Gasanova L. G. Structural and optical properties of Ga_2Se_3 crystals by spectroscopic ellipsometry. *Journal of Electronic Materials*. 2019;48: 2418. https://doi.org/10.1007/s11664-019-07000-4

22. Morley S., Emde M., Zahn D. R. T., ... Poole I. B. Optical spectroscopy of epitaxial Ga_2Se_3 layers from the far infrared to the ultraviolet. *Journal of Applied Physics*. 1996;79: 3196–3199. https://doi.org/10.1063/1.361264

23. El-Rahman K. F. Charge conduction mechanisms and photovoltaic properties of n-(Ga_2S_3 – Ga_2Se_3)/p-Si heterojunctions. *The European Physical Journal Applied Physics*. 2007;37(2): 143–147. https://doi.org/10.1051/epjap:2007004

24. Kuzubov S. V., Kotov G. I., Synorov, Yu. V. Gallium vacancy ordering in Ga_2Se_3 thin layers on Si(100), Si(111), and Si(123) substrates. *Crystallography Reports*. 2017;62(5): 768–772. https://doi.org/10.1134/s1063774517050121

25. Budanov A. V., Vlasov Y. N., Kotov G. I., Rudnev E. V., Mikhailyuk E. A. Deep levels in Ga_2Se_3/GaP (111) heterostructures. *Chalcogenide Letters*. 2018;15(8): 425–428. Available at: https://chalcogen.ro/425_BudanovAV.pdf

26. Budanov A. V., Vlasov Yu. N., Kotov G. I., Burtsev A. A., Rudnev E. V. Photosensitivity of In_2Se_3/InAs heterostructures[*]. In: *Actual problems in micro- and nanoelectronics*. Interuniversity collection of scientific papers: Voronezh-2022. 2022: 24–30. (In Russ.). Available at: https://catalog.inforeg.ru/Inet/GetEzineByID/33862

27. Bezryadin N. N., Kotov G. I., Kubuzov S. V., Vlasov Yu. N. Surface phase of Ga_2Se_3 on GaP (111). *Condensed Matter and Interfaces*. 2013;15: (4): 382–386. (In Russ., abstract in Eng.). Available at: https://elibrary.ru/item.asp?id=20931229

28. Pardo M., Tomas A., Guittard M. Polymorphisme de Ga_2S_3 et diagramme de phase Ga – S. *Materials Research Bulletin*. 1987;22(12): 1677–1684. https://doi.org/10.1016/0025-5408(87)90011-0

29. Pardo M., Guittard M., Chilouet A., Tomas A. Diagramme de phases gallium – soufre et etudes structurales des phases solides. *Journal of Solid State Chemistry*. 1993;102(2): 423–433. https://doi.org/10.1006/jssc.1993.1054

30. Volkov V. V., Sidey V. I., Naumov A. V., ... Zavrazhnov A. Yu. Structural identification and stabilization of the new high-temperature phases in A(III) – B(VI) systems (A = Ga, In, B = S, Se). Part 1: High-temperature phases in the Ga – S system. *Journal of Alloys and Compounds*. 2022;899: 163264. https://doi.org/10.1016/j.jallcom.2021.163264

31. Ho C. H. Ga_2Se_3 defect semiconductors: the study of direct band edge and optical properties. *ACS Omega*. 2020;29(5): 18527–18534. https://doi.org/10.1021/acsomega.0c02623

32. Shi C., Yang B., Hu B., Du1 Y., Yao S. Thermodynamic description of the Al–X (X = S, Se, Te) systems. *Journal of Phase Equilibria and Diffusion*. 2019;40: 392–402. https://doi.org/10.1007/s11669-019-00733-z

33. Chen G., Drennan Z. G., Zou J. Indium selenides: structural characteristics, synthesis and their thermoelectric performances. *Small*. 2014;14(10): 2747–2765. https://doi.org/10.1002/smll.201400104

34. Brezhnev N. Y., Dorokhin M. V., Zavrazhnov A. Y., Kolyshkin N. A., Nekrylov I. N., Trushin V. N. High-temperature gallium sesquisulfides and a fragment of the *T-x* diagram of the Ga – S system with these phases. *Condensed Matter and Interphases*. 2024;26(2):225–237. https://doi.org/10.17308/kcmf.2024.26/11936

35. Likforman A., Fourcroy P.-H., Guittard M., Flahaut J., Poirier R., Szydlo N. Transitions de la forme de haute température α de In_2Se_3, de part et d'autre de la température ambiante. *Journal of Solid State Chemistry*. 1980;33(1): 91–97. https://doi.org/10.1016/0022-4596(80)90551-4

36. Davydov S. Yu., Kobyakov I. B. Dependence of elastic constants of zinc sulfide on the phase composition of wurtzite/sphalerite*. *Soviet Physics: Thechnical Physics*. 1983;53(2): 377–379. (In Russ.). Available at: https://www.mathnet.ru/php/archive.phtml?wshow=paper&jrnid=jtf&paperid=2201&option_lang=rus

37. Brezhnev N. Yu. Ga-S and In-Se systems: crystal structure of intermediate phases and *T-x* diagrams*. Cand. chem. sci. diss. Voronezh, 2023. 189 p. Available at: https://rusneb.ru/catalog/000199_000009_012131968/

38. Lutz D, Fischer M., Baldus H.-P., Blachnik R. Zur polymorphie des In_2Se_3. *Journal of the Less Common Metals*. 1988;143: 83–92. https://doi.org/10.1016/0022-5088(88)90033-1

39. Pfitzner A., Lutz H. D. Redetermination of the crystal structure of γ-In_2Se_3 by twin crystal X-ray method. *Journal of Solid State Chemistry*. 1996;124: 305–308. https://doi.org/10.1006/jssc.1996.0241

40. Manolikas C. New results on the phase transformations of In_2Se_3. *Journal of Solid State Chemistry*. 1988;74: 319–328. https://doi.org/10.1016/0022-4596(88)90361-1

41. Landuyt J., Tendeloo G., Amelinckx S. Phase transitions in In_2Se_3 as studied by electron microscopy and electron diffraction. *Physica Status Solidi (a)*. 1975;30: 299–302. https://doi.org/10.1002/pssa.2210300131

42. Ye J., Yoshida T, Nakamura Y.; Nittono O. Optical activity in the vacancy ordered III_2VI_3 compound semiconductor $(Ga_{0.3}In_{0.7})_2Se_3$. *Applied Physics Letters*. 1995;67(21): 3066–3068. https://doi.org/10.1063/1.114866

43. Kojima N., Morales C., Ohshita T., Yamaguchi M. Ga_2Se_3 and $(InGa)_2Se_3$ as novel buffer layers in the GaAs on Si system. *AIP Conference Proceedings*. 2013;1556(1): 38–40. https://doi.org/10.1063/1.4822194

44. Küpers M., Konze P. M., Meledin A., ... Dronskowski R. Controlled crystal growth of indium selenide, In_2Se_3, and the crystal structures of α-In_2Se_3. *Inorganic Chemistry*. 2018;57(18): 11775–11781. https://doi.org/10.1021/acs.inorgchem.8b01950

45. Popovic S., Celustka B., Bidjin D. X-ray diffraction measurement of lattice parameters of In_2Se_3. *Physica Status Solidi (a)*. 1971;6(1): 301–304. https://doi.org/10.1002/pssa.2210060134

46. Likforman A., Guittard M., Tomas A., Mise en evidence d'une solution de type spinelle dans le diagramme de phase du systeme In – S. *Journal of Solid State Chemistry*. 1980;34(3): 353–359. https://doi.org/10.1016/0022-4596(80)90434-X

47. Kosyakov A. V., Zavrazhnov A. Yu., Naumov A. V. Refinement of the In-S phase diagram using spectrophotometric characterization of equilibria between hydrogen and indium sulfides. *Inorganic Materials*. 2010;46(4): 343–345. https://doi.org/10.1134/s0020168510040035

48. Kosyakov A. V., Zavrazhnov A. Y., Naumov A. V., Sergeyeva A. V. Specification of the phase diagram of system In - S according to spectrophotometric researches of balance between sulfide of indium and hydrogen. *Proceedings of Voronezh State University. Series: Chemistry. Biology. Pharmacy". Series: Chemistry. Biology. Pharmacy*. 2009;2: 28–39. (In Russ., abstract in Eng.). Available at: https://elibrary.ru/item.asp?id=12992199

49. Zavrazhnov A. Y., Naumov A. V., Anorov P. V., ... Pervov V. S. *T-x* phase diagram of the In-S system. *Inorganic Materials*. 2006:42: 1294–1298. https://doi.org/10.1134/S0020168506120028

50. Naumov A. V., Sergeeva A. V., Semenov V. N. Structure and reflection spectra of $In_{3-x}S_4$(111)/mono-Si and $In_{3-x}S_4$(111)/SiO_2/mono-Si films. *Inorganic Materials*. 2015;51(12): 1205–1212. https://doi.org/10.1134/S0020168515110060

51. Naumov A. V., Sergeeva A. V., Semenov V. N. Oriented $In_{3-x}S_4$ films on the (100) surface of Si, GaAs, and InP single crystals. *Inorganic Materials*. 2017;53(6): 560–567. https://doi.org/10.1134/S0020168517060127

52. Pistor P., Alvarez J. M., Leon M., di Michiel M. Structure reinvestigation of α-, β- and γ-In_2S_3. *Acta Crystallographica Section B Structural Science, Crystal Engineering and Materials*. 2016;72(3): 410–415. https://doi.org/10.1107/S2052520616007058

53. Bartzokas D., Manolikas C. Spyridelis J. Electron microscopic study of the destabilization of stabilized γ-phase of indium sesquisulphide. *Physica Status Solidi (a)*. 1978;47(2): 459–467. https://doi.org/10.1002/pssa.2210470216

54. Diehl R., Carpentier C. D., Nitsche R. The crystal structure of γ-In_2S_3 stabilized by As or Sb. *Acta Crystallographica Section B Structural Crystallography and Crystal Chemistry*. 1976;32(4): 1257–1260. https://doi.org/10.1107/s0567740876005062

55. Liu K., Dai L., Li H., Hu H, ... Hong M. Evidences for phase transition and metallization in β–In_2S_3 at high pressure. *Chemical Physics*. 2019;524: 63–69. https://doi.org/10.1016/j.chemphys.2019.04.025

56. Jebasty R. M., Sjastad A. O., Vidya R. Prediction of intermediate band in Ti/V doped γ-In_2S_3. *RSC Advances*. 2022;12(3): 1331–1340. https://doi.org/10.1039/d0ra08132a

57. Berezin S. S., Berezina M. V., Zavrazhnov A. Yu., Kosyakov A. V., Sergeeva A. V., Sidei V. I. Phase transformations of indium mono- and sesquisulfides studied by a novel static thermal analysis technique. *Inorganic Materials*. 2013;49(6): 555–563. https://doi.org/10.1134/S0020168513060010

58. Zavrazhnov A. Y., Kosyakov A. V., Naumov A. V., Sergeeva A. V., Berezin S. S. Study of the In-S phase diagram using spectrophotometric characterization of equilibria between hydrogen and indium sulfides. *Thermochimica Acta*. 2013;566(20): 169–174. https://doi.org/10.1016/j.tca.2013.05.031

59. Depeursinge Y., Electronic properties of the layer III–VI semiconductors. A comparative study. *Il Nuovo*

Cimento B Series 11. 1981;64: 111–150. https://doi.org/10.1007/BF02721299

60. Jie W., Hao J. Two-dimensional layered gallium selenide: preparation, properties and applications. In: *Advanced 2D Materials*. Tiwari A., Syväjärvi M. (eds.). New York: Wiley; 2016: 1–36. 514 p. https://doi.org/10.1002/9781119242635.ch1

61. Schluter M., Camassel J., Kohn S., ... Cohen M. L. Optical properties of GaSe and GaS_xSe_{1-x} mixed crystals. *Physical Review B*. 1976;13(8): 3534–3547. https://doi.org/10.1103/PhysRevB.13.3534

62. Liu F., Shimotani H., Shang H., ... Drummond N. High-sensitivity photodetectors based on multilayer GaTe flakes. *ACS Nano*. 2014;8(1): 752–760. https://doi.org/10.1021/nn4054039

63. Edwards D. F. Gallium telluride (GaTe). In: *Handbook of Optical Constants of Solids*. Palik E. D. (ed.). Amsterdam: Elsevier; 1997. p. 489–505. https://doi.org/10.1016/b978-012544415-6/50114-x

64. Grygorchak I., Voitovych S., Stasyuk I., Velychko O., Menchyshyn O. Electret effect in intercalated crystals of the $A^{III}B^{VI}$ group. *Condensed Matter Physics*. 2007;10(1): 51–60. https://doi.org/10.5488/CMP.10.1.51

65. Rajapakse M., Karki B., Abu U. O.,...Yu M. Intercalation as a versatile tool for fabrication, property tuning, and phase transitions in 2D materials. *Npj 2D Materials and Applications*. 2021;5: Article-30. https://doi.org/10.1038/s41699-021-00211-6

66. Nekrasov O. V., Zavrazhnov A. Yu., Semenov, V. N. Dolgopolova E. A., Averbakh E. M. Incorporation of HNO_3 into GaSe and InSe*. *Inorganic Materials* 1994;30(6): 737–740. (In Russ.). Available at: https://elibrary.ru/item.asp?id=28934301

67. Zavrazhnov A. Yu., Turchen D. N., Semenov V. N. Zlomanov V. P, Pervov V. S. Oxidizing intercalation of layered structures. *Materials Technology*. 2000;15(2): 155–160. https://doi.org/10.1080/10667857.2000.11752872

68. Zavrazhnov A. Yu., Nekrasov O. V., Averbakh E. M. Falkengof A. T. On the possibility of insertion of some organic molecules into GaSe and InSe*. *Inorganic Materials*. 1994;30(6): 1030–1032. (In Russ.). Available at: https://elibrary.ru/item.asp?id=29831583

69. Vela Y. G., Juan D., Dicorato S., Losurdo M. Layered gallium sulfide optical properties from monolayer to CVD crystalline thin films. *Optics Express*, 2022;30: 15. https://doi.org/10.1364/OE.459815

70. Zavrazhnov A. Yu., Turchen D. N. Oxidative insertion into GaSe-type structures*. *Condensed Matter and Interphase*. 1999;1(2): 190–196. (In Russ.). Available at: https://www.elibrary.ru/item.asp?id=24120596

71. Motter J. P., Koski K. J. Cui Y. General strategy for zero-valent intercalation into two-dimensional layered nanomaterials. *Chemistry of Materials*. 2014;26: 2313–2317. https://doi.org/10.1021/cm500242h

72. Turchen D. N., Zavrazhnov A. Yu., Goncharov E. G., Suvorov A.V . Nonstoichiometry research for the low-volatilaty phases. Homogeneity region of GaSe*. *Russian Journal of General Chemistry*. 1998;68(6): 920–925. (In Russ.). Available at: https://elibrary.ru/ynceoh

73. Turchen D. N., Zavrazhnov A. Yu., Prigorodova T. V. Scanning of *T-x*-projections of phase microdiagrams based on the gas solubility in melts*. *Russian Journal of General Chemistry*. 1999;69(5): 1–8. (In Russ.).

74. Ikram R., Jan B. M., Ahmad W. An overview of industrial scalable production of graphene oxide and analytical approaches for synthesis and characterization. *Journal of Materials Research and Technology*. 2020;9(5): 11587–11610. https://doi.org/10.1016/j.jmrt.2020.08.050

75. Julien C., Nazri G. A. Intercalation compounds for advanced lithium batteries. Chapter 3. In: *Handbook of Advanced Electronic and Photonic Materials and Devices*. H. S. Nalwa (ed.). USA. Academic Press; 2001;10: 99–181. https://doi.org/10.1016/b978-012513745-4/50083-4

76. Ng B., Wong C., Niu W., ... Tsang S. Molecular layer-by-layer re-stacking of MoS_2–In_2Se_3 by electrostatic means: assembly of a new layered photocatalyst. *Materials Chemistry Frontiers*. 2023;7(5): 937–945. https://doi.org/10.1039/D2QM01095J

77. Karpov V. V., Bandura A. V., Evarestov R. A. Nonempirical calculations of the structure and stability of nanotubes based on gallium monochalcogenides. *Physics of the Solid State*. 2020;62(6): 1017–1023. https://doi.org/10.1134/S1063783420060116

78. Xu K., Yin L., Huang Y. Synthesis, properties and applications of 2D layered $M^{III}X^{VI}$ (M = Ga, In; X = S, Se, Te) materials. *Nanoscale*. 2016;8(38): 16802-16818. https://doi.org/10.1039/C6NR05976G

79. Abd-Elkader O. H., Abdelsalam H., Sakr M. A., Teleb N. H., Zhang Q. Electronic and optical properties of finite gallium sulfide nano ribbons: a first-principles study. *Crystals*. 2023;1215: 13. https://doi.org/10.3390/cryst13081215

80. Ren D., Merdrignac-Conanec O., Dorcet V., ... Zhang X. *In situ* synthesis and improved photoelectric performances of a Sb_2Se_3/β-In_2Se_3 heterojunction composite with potential photocatalytic activity for methyl orange degradation. *Ceramics International*. 2020;46(16): 25503–25511. https://doi.org/10.1016/j.ceramint.2020.07.021

81. Ambrosi A., Pumera A. Exfoliation of layered materials using electrochemistry. *Chemical Society Reviews*. 2018;47: 7213–7224. https://doi.org/10.1039/c7cs00811b

82. Wang T., Wang J., Wu J., Ma P., Su R., Zhou P. Near-infrared optical modulation for ultrashort pulse generation employing indium monosulfide (InS) two-dimensional semiconductor nanocrystals. *Nanomaterials*. 2019;9: 865. https://doi.org/10.3390/nano9060865

83. Shao M., Bie T., Yang L., ... He L. Over 21% efficiency stable 2D perovskite solar cells *Advanced Materials*. 2022;34: 2107211. https://doi.org/10.1002/adma.202107211

84. Harvey A., Backes C., Gholamvand Z., Hanlon D., McAteer D. Preparation of gallium sulfide nanosheets by liquid exfoliation and their application as hydrogen evolution catalysts. *Chemistry of Materials*. 2015;27: 3483–3493. https://doi.org/10.1021/acs.chemmater.5b00910

85. Zhang C., Park S. H., Ronan O. ... Nicolosi V. Enabling flexible heterostructures for Li-ion battery an-odes based on nanotube and liquid-phase exfoliated 2D gallium chalcogenide nanosheet colloidal solutions. *Small*, 2017;13(34): 1701677. https://doi.org/10.1002/smll.2017016

86. Ahmed S., Cheng P.K., Qiao J. Nonlinear optical activities in two-dimensional gallium sulfide: a comprehensive study. *ACS Nano*. 2022;16(8): 12390–12402 https://doi.org/10.1021/acsnano.2c03566

87. Zappia M. I., Bianca G., Bellani S., Curreli N. Two-dimensional gallium sulfide nanoflakes for UV-selective photoelectrochemical-type photodetectors. *The Journal of Physical Chemistry C*. 2021;125(22):11857–11866. https://doi.org/10.1021/acs.jpcc.1c03597

88. Opoku F., Akoto O., Asare-Donkor N. K., Adimado A. A. Defect-engineered two-dimensional layered gallium sulphide molecular gas sensors with ultrahigh selectivity and sensitivity. *Applied Surface Science*. 2021;562: 150188. https://doi.org/10.1016/j.apsusc.2021.150188

89. Lu Y., Warner J. H. Synthesis and applications of wide bandgap 2D layered semiconductors reaching the green and blue wavelengths. *ACS Applied Electronic Materials*. 2020;7(2): 1777–1814. https://doi.org/10.1021/acsaelm.0c00105

90. Côté M., Cohen M. L., Chadi J. D. GaSe nanotubes. *Physical Review B*. 1998;58: R4277. https://doi.org/10.1103/PhysRevB.58.R4277

91. Seral-Ascaso A., Metel S., Pokle A. Long-chain amine-templated synthesis of gallium sulfide and gallium selenide nanotubes. *Nanoscale*. 2016;8: 11698–11706. https://doi.org/10.1039/C6NR01663D

92. Petroni E., Lago E., Bellani S. Liquid-phase exfoliated indium-selenide flakes and their application in hydrogen evolution reaction. *Small*. 2018;26(14): e1800749. https://doi.org/10.1002/smll.201800749

93. Shi G., Kioupakis E. Anisotropic spin transport and strong visible-light absorbance in few-layer SnSe and GeSe. *Nano Letters*. 2015;15:6926. https://pubs.acs.org/doi/10.1021/acs.nanolett.5b02861

94. Wasala M., Sirikumara H. I., Raj Sapkota Y., ... Talapatra S. Recent advances in investigations of the electronic and optoelectronic properties of group III, IV, and V selenide based binary layered compounds. *Journal of Materials Chemistry C*. 2017;43(5): 11214–11225. https://pubs.acs.org/10.1039/c7tc02866k

95. Yüksek M., Elmali A., Karabulut M. Nonlinear absorption in undoped and Ge doped layered GaSe semiconductor crystals. *Applied Physics B*. 2010;98: 77–81. https://doi.org/10.1007/s00340-009-3665-y

96. Zhou X., Cheng J., Zhou Y., ... Yu D. Strong second-harmonic generation in atomic layered GaSe. *American Chemical Society*. 2015;137(25): 7994–7997. https://doi.org/10.1021/jacs.5b04305

97. Hu L., Huang X., Wei D. Layer-independent and layer-dependent nonlinear optical properties of two-dimensional GaX (X = S, Se, Te) nanosheets. *Physical Chemistry Chemical Physics*. 2017;19(18): 11131–11141. https://doi.org/10.1039/c7cp00578d

98. Gan X. T., Zhao C., Hu S. Microwatts continuous-wave pumped second harmonic generation in few- and mono-layer GaSe. *Light: Science and Applications*. 2018;7: 17126. https://doi.org/10.1038/lsa.2017.126

99. Karatay A., Yuksek M., Ertap H., Elmali A., Karabulut M. Enhancing the blue shift of SHG signal in GaSe:B/Ce crystal. *Optics and Laser Technology*. 2018;99: 392–395. https://doi.org/10.1016/j.optlastec.2017.09.027

100. Yuan Q., Fang L., Fang H., ... Gan X. Second harmonic and sum-frequency generations from a silicon metasurface integrated with a two-dimensional material. *ACS Photonics*. 2019;6: 2252–2259. https://doi.org/10.1021/acsphotonics.9b00553

101. Fernelius N. Properties of gallium selenide single crystal. *Progress in Crystal Growth and Characterization of Materials*. 1994;28(4): 275–353. https://doi.org/10.1016/0960-8974(94)90010-8

102. Sarkisov S. Yu., Mikhailov T. A., Bereznaya S. A., Korotchenko Z. V., Redkin R. A. *Nonlinear optical element based on a GaSe single crystal with a double-sided antireflection coating for generating terahertz radiation*[*]. Patent RF: No. 193143U1. Publ. 15.10.2019, bull. No. 29. (In Russ.) Available at: https://patents.google.com/patent/RU193143U1/ru

103. Lubenko D. M., Ezhov D. M., Losev V. F., Andreev Yu. M., Lanskii G. V. IR-to-THz down conversion in nonlinear GaSe:Al crystals. *Bulletin of the Russian Academy of Sciences: Physics*. 2020;84(7): 780–782. https://doi.org/10.3103/s1062873820070163

104. Kul'chitskii N. A., Naumov A. V. Modern state of markets of selenium and selenium-based compounds. *Izvestiya Vuzov. Tsvetnaya Metallurgiya (Proceedings of Higher Schools. Nonferrous Metallurgy)*. 2015;3: 40–48. https://doi.org/10.17073/0021-3438-2015-3-40-48

105. Gershenzon E. G. Submillimeter spectroscopy[*]. *Sorosovskij obrazovatel'nyj zhurnal. Serija Fizika. Physics Series*. 1998;4: 78–85. (In Russ.). Avalable at: https://www.pereplet.ru/obrazovanie/stsoros/533.html

106. Song M., An N., Zou Y. Epitaxial growth of 2D gallium selenide flakes for strong nonlinear optical response and visible-light photodetection. *Frontiers of Physics*. 2023;18: 52302. https://doi.org/10.1007/s11467-023-1277-3

107. Yan D., Xu D., Wang Y., Zhong K., Tunable J. High-repetition-rate, tunable and coherent mid-infrared source based on difference frequency generation from a dual-wavelength 2 μm laser and GaSe crystal. *Laser Physics*. 2018;28(12): 126205. https://doi.org/10.1088/1555-6611/aae060

108. Rao Z., Wang X., Lu Y. Tunable terahertz generation from one CO_2 laser in a GaSe crystal. *Optics Communications*. 2011;23(284): 5472–5474. https://doi.org/10.1016/j.optcom.2011.08.009

109. Gamal G. A., Azad M. A. Photoelectric studies of gallium monosulfide single crystals. *Journal of Physics and Chemistry of Solids*. 2005;66(1): 5–10. https://doi.org/10.1016/j.jpcs.2004.06.011

110. Qasrawi A. F., Gasanly N. M. Carrier transport properties of InS single crystals. *Crystal Research and Technology*. 2002;37: 1104. https://doi.org/10.1002/1521-4079(200210)37:10<1104::AID-CRAT1104>3.0.CO;2-A

111. Ayddinli A., Gasanly N. M., Uka A. Anharmonicity in GaTe layered crystals. *Crystal Research and Technology*. 2002;37(12): 1303–1309. https://doi.org/10.1002/crat.200290006

112. Ahmad H., Azali N., Yusoff N. Layered gallium telluride for inducing mode-locked pulse laser in thulium/

holmium-doped fiber. *Luminescence*, 2022;248: 119002. https://doi.org/10.1016/j.jlumin.2022.119002

* *Translated by author of the article*

Information about the authors

Alexander Y. Zavrazhnov, Dr. Sci. (Chem.), Professor at the Department of General and Inorganic Chemistry, Voronezh State University (Voronezh, Russian Federation).
https://orcid.org/0000-0003-0241-834X
alexander.zavrazhnov@gmail.com

Nikolay Y. Brezhnev, Junior Researcher at the Department of Chemistry, Voronezh State Agricultural University (Voronezh, Russian Federation).
https://orcid.org/0000-0002-3287-8614
brezhnevnick@gmail.com

Ivan N. Nekrylov, Department Assistant at the Department of General and Inorganic Chemistry, Voronezh State University (Voronezh, Russian Federation).
https://orcid.org/0000-0003-4491-4739
Icq492164858@gmail.com

Andrew V. Kosyakov, Cand. Sci. (Chem.), Assistant Professor, Department of General and Inorganic Chemistry, Voronezh State University (Voronezh, Russian Federation).
https://orcid.org/0000-0001-9662-7091.
lavchukb@mail.ru

Viktor F. Kostryukov, Dr. Sci. (Chem.), Associate Professor, Associate Professor at the Department of Materials Science and the Industry of Nanosystems, Voronezh State University (Voronezh, Russian Federation).
https://orcid.org/0000-0001-5753-5653
vc@chem.vsu.ru

Received 28.07.2024; approved after reviewing 18.08.2024; accepted for publication 16.09.2024; published online 25.12.2024.

Translated by Valentina Mittova